

THE NONTHERMAL ROTATIONAL DISTRIBUTION OF H_3^+

TAKESHI OKA

Department of Astronomy and Astrophysics, Department of Chemistry, and The Enrico Fermi Institute,
University of Chicago, Chicago, IL 60637; t-oka@uchicago.edu

AND

ERIK EPP

Department of Chemistry and The Enrico Fermi Institute, University of Chicago, Chicago, IL 60637

Received 2004 April 29; accepted 2004 June 4

ABSTRACT

Although H_3^+ is nonpolar in the equilateral triangle equilibrium structure, symmetry breakdown due to centrifugal distortion causes a small dipole moment and hence rotational transitions. The spontaneous emission times are on the order of a few weeks for low rotational levels and are comparable to collision intervals in interstellar space. Moreover, there are metastable rotational levels such as $J = K = 3$, from which spontaneous emissions are rigorously forbidden. A very nonthermal rotational distribution is produced. We present a model calculation simulating the thermalization of H_3^+ . Since the lifetime of H_3^+ in interstellar space is orders of magnitude longer than the spontaneous emission time and collision intervals, a steady state approximation is assumed. Accurate theoretical values by ab initio theory are used for spontaneous emission rates. The rates of collision-induced transitions between rotational levels are calculated on the assumption of completely random selection rules using an approximate formula that satisfies the principle of detailed balancing. The results indicate that the observed high population of H_3^+ in the (3, 3) metastable level toward the Galactic center (M. Goto and coworkers) signifies the presence of very large high-temperature ($T \geq 300$ K) and low-density [$n(\text{H}_2) \leq 70 \text{ cm}^{-3}$] clouds. It is shown that other higher metastable levels may accommodate observable H_3^+ in such clouds and that the excitation temperature determined from the observed relative populations of (1, 0) and (1, 1) should provide crucial information on the condition of such clouds.

Subject headings: astrochemistry — infrared: ISM — ISM: lines and bands — ISM: molecules — molecular processes

1. INTRODUCTION

Recent infrared spectroscopic observations of H_3^+ have established the remarkable ubiquity of this fundamental molecular ion, which acts as a universal proton donor (acid) and initiates interstellar chemistry (Herbst & Klemperer 1973; Watson 1973). H_3^+ with column densities on the order of 10^{14} cm^{-2} has been detected not only in dense molecular clouds with high extinctions ($A_V \sim 100$; Geballe & Oka 1996; McCall et al. 1999), where its abundance had been anticipated from chemical model calculations, but also in diffuse clouds with lower extinctions. Examples include those toward Cygnus OB2 12 ($A_V \sim 10$; McCall et al. 1998; Geballe et al. 1999) and the classic translucent sight line HD 183143 ($A_V \sim 4$; McCall et al. 2002), and the unexpectedly high abundance has introduced an enigma into the chemistry of the diffuse interstellar medium. The recent discovery of H_3^+ toward the bright star ζ Per ($A_V \sim 1$) is particularly noteworthy (McCall et al. 2003). This ubiquity of H_3^+ in clouds with a wide range of extinctions makes it a unique general probe for studying astrophysical molecular plasmas. These observations were all done using the three absorption lines $R(1, 1)^u$, $R(1, 0)$, and $R(1, 1)^l$, starting from the lowest two rotational levels, i.e., the $(J, K) = (1, 1)$ level of para- H_3^+ and the (1, 0) level of ortho- H_3^+ , which is 32.9 K above (1, 1).

Recently, a new absorption line, $R(3, 3)^l$, at 2829.925 cm^{-1} was observed toward the Galactic center sources GCS 3-2 and GC IRS 3 at the Subaru Telescope (Goto et al. 2002) and was confirmed at UKIRT (T. R. Geballe 2003, private

communication). The intense observed spectral line demonstrates that the metastable (3, 3) rotational level (see below), despite being higher than the lowest (1, 1) level by as much as 361.5 K, has a population of H_3^+ comparable to that in (1, 1). On the other hand, our attempt at detecting the $R(2, 2)^l$ absorption line at 2762.070 cm^{-1} was not successful, and its upper limit indicates that the (2, 2) level, which is only 151.3 K higher than (1, 1), has a population lower than (3, 3) by at least a factor of 5. In this paper we study the molecular processes that lead to this remarkable, nonthermal rotational distribution of H_3^+ .

2. METASTABLE ROTATIONAL LEVELS OF H_3^+

In weakly ionized plasmas of dense and diffuse clouds, the radiative temperature (2.7 K) is much lower than the kinetic temperature, and this causes nonthermal molecular distributions. The rotational excitation temperature is determined from a balance between spontaneous emission processes, which follow rigorous selection rules, and collisional processes, which do not follow selection rules as rigorously (Oka 1973). For example, if the cloud density is comparable to critical densities, the rotational distribution of CO is determined from a balance of the spontaneous emission that follows the $\Delta J = -1$ rule and the collisional excitation and de-excitations that do not follow selection rules as rigorously (Green & Chapman 1978). This may lead to a very nonthermal rotational distribution of CO, including population inversion (Goldsmith 1972). The situation is more subtle for H_3^+ because of its special mechanism of spontaneous emissions (Pan & Oka 1986), with critical

densities comparable to cloud densities. H_3^+ also differs from ordinary molecules in that its collisions with H_2 are reactive collisions with a large Langevin rate and occur almost randomly, without selection rules.

The rotational energy levels of H_3^+ in the ground vibrational state are shown in Figure 1, in which the levels are specified by the rotational quantum number J , its projection to the C_3 symmetry axis K , and the parity, plus or minus, which is determined by $(-1)^K$. This is a typical energy level pattern for an oblate, symmetric, top molecule. Levels with $K = 3n$, shown by thick lines, are occupied by ortho- H_3^+ , with a total nuclear spin quantum number $I = 3/2$, while those with $K = 3n \pm 1$, shown by thin lines, are occupied by para- H_3^+ , with $I = 1/2$. The eigenfunctions for the levels shown with dashed lines, (0, 0), (2, 0), and (4, 0), are totally symmetric and cannot accommodate three protons according to the Pauli exclusion principle, just as s -orbitals of atoms cannot accommodate more than two electrons.

Being an equilateral triangle, H_3^+ in its equilibrium structure does not have a permanent dipole moment. However, rotation of the molecule breaks the D_{3h} symmetry by centrifugal distortion and produces a small dipole moment, which induces normally forbidden rotational transitions (Watson 1971). Spontaneous emission due to this effect was first considered for the thermalization of interstellar NH_3 by Oka et al. (1971). The spontaneous emission is much more significant for H_3^+ than for NH_3 for two reasons (Pan & Oka 1986): (1) Unlike NH_3 , which has a large permanent dipole moment of 1.468 D, the symmetry-breaking dipole moment on the order of 10^{-2} D is the only mechanism of spontaneous emission for H_3^+ . (2) In addition, because H_3^+ (with rotational constant $B = 43.6 \text{ cm}^{-1}$) is much lighter than NH_3 ($B = 9.94 \text{ cm}^{-1}$), both the transition moment, which is proportional to B^3 , and the ν^3 factor in the Einstein coefficient for spontaneous emission are much larger for H_3^+ . Thus, for example, the lifetime of the (2, 2) \rightarrow (1, 1) emission is 7.3×10^9 s (320 yr) for NH_3 (Oka et al. 1971) but is only 2.35×10^6 s (27.2 days) for H_3^+ (Neale et al. 1996). The latter timescale is comparable to that of collisions and causes a nonthermal distribution.

The spontaneous emission of H_3^+ obeys the selection rules of the ordinary kind: $\Delta J = 0, \pm 1$, parity $+\leftrightarrow -$, and ortho \leftrightarrow para ($\Delta I = 0$), and, in addition, $\Delta k = \pm 3$, where k is the signed quantum number of K (Pan & Oka 1986). The last rule is required so that the transition moment is invariant with respect to the (123) permutation of the protons. (In principle, $\Delta k = \pm 9, \pm 15$, etc., are also allowed from symmetry arguments alone, but they are so much weaker than the $\Delta k = \pm 3$ transitions that we can neglect them for all practical purposes.) The aforementioned (2, 2) \rightarrow (1, 1) transition, which formally looks like $\Delta K = 1$, is actually $\Delta k = \pm 3$ for $k = \pm 2 \rightarrow \mp 1$. Spontaneous emissions allowed by the selection rules are shown in Figure 1 (arrows). Note that ortho- H_3^+ in the (1, 0), (3, 3), and (6, 6) levels and para- H_3^+ in the (5, 5) level cannot emit spontaneously. We call them “metastable levels” and show them with shaded lines in Figure 1. We see from the absolute values of the rotational energy (Lindsay & McCall 2001) that $J = K$ levels with $J > 4$ and $J = K + 1$ levels with $J > 7$ are metastable because they do not have lower rotational levels for making transitions that obey the selection rules. The (4, 4) level is nearly metastable since it is only 7.275 cm^{-1} above the (3, 1) level, and its spontaneous emission lifetime is long (11 yr); we can call it a “quasi-metastable level.” Black (1998) has speculated that the (4, 4) \rightarrow (3, 1) emission may cause an interstellar H_3^+ maser.

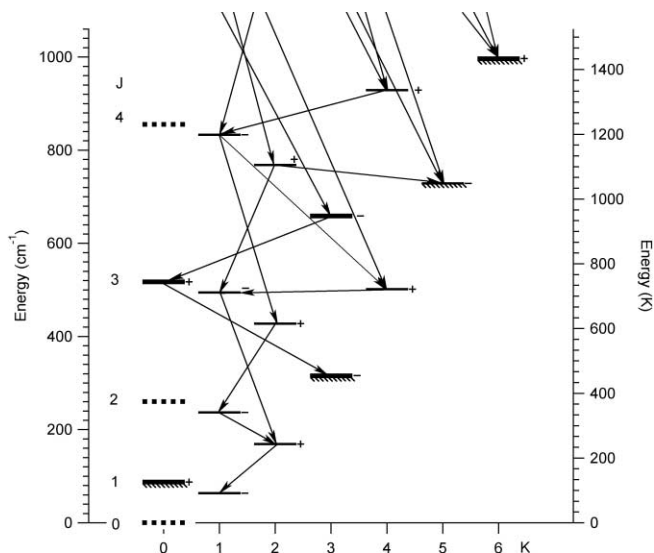


FIG. 1.—Rotational energy levels of H_3^+ in the ground vibrational state. Levels of ortho- H_3^+ ($K = 3n$) and para- H_3^+ ($K = 3n \pm 1$) are shown by thick and thin lines, respectively, with parities $(-1)^K$ indicated with a plus or minus sign. The (0, 0), (2, 0), and (4, 0) levels shown with dotted lines are forbidden by the Pauli exclusion principle. The (1, 0), (3, 3), (5, 5), and (6, 6) levels shown with hatched lines are the metastable levels from which spontaneous emissions are forbidden. Spontaneous emissions are shown by arrows.

The population inversion for the two levels is nearly perfect for low-density clouds since the lifetime of the (3, 1) \rightarrow (2, 2) emission is only ~ 8 hr.

3. THERMALIZATION

In dense clouds, the main destruction process of H_3^+ is proton hop reactions, $\text{H}_3^+ + \text{X} \rightarrow \text{HX}^+ + \text{H}_2$, where X is mainly CO and O, while in diffuse clouds it is dissociative recombination with electrons, $\text{H}_3^+ + e^- \rightarrow \text{H} + \text{H} + \text{H}$ or $\text{H}_2 + \text{H}$. Since the former has a Langevin rate constant of $k_L \sim 2 \times 10^{-9} \text{ cm}^3 \text{ s}^{-1}$ (Anicich & Huntress 1986) and the latter $k_e \sim 2 \times 10^{-7} \text{ cm}^3 \text{ s}^{-1}$ (McCall et al. 2003), the lifetime of H_3^+ is estimated to be $t \sim [k_{\text{CO}}n(\text{CO})]^{-1} \sim 3 \times 10^8$ s in typical dense clouds with a CO density $n(\text{CO}) \sim 1.5 \text{ cm}^{-3}$, and $t \sim [k_e n(e^-)]^{-1} \sim 3 \times 10^8$ s also in typical diffuse clouds, with an electron density of $n(e^-) \sim 1.5 \times 10^{-2} \text{ cm}^{-3}$.

Those lifetimes are much longer than the times of both spontaneous emission and collision. Assuming a Langevin rate constant of $2 \times 10^{-9} \text{ cm}^3 \text{ s}^{-1}$, we note the average collision interval to be $\sim 5 \times 10^4$ s for dense clouds with $n(\text{H}_2) \sim 10^4 \text{ cm}^{-3}$ and $\sim 5 \times 10^6$ s for diffuse clouds with $n(\text{H}_2) \sim 10^2 \text{ cm}^{-3}$. Thus, H_3^+ collides with H_2 approximately 10^4 and 10^2 times during its life in dense and diffuse clouds, respectively. These numbers do not depend critically on the assumed value of $n(\text{H}_2)$, since both $n(\text{CO})$ and $n(e^-)$ scale with $n(\text{H}_2)$ for typical dense and diffuse clouds, where H_3^+ abounds. This allows us to use the steady state approximation in § 3.3.

3.1. Radiative Process

The rate of spontaneous emission of H_3^+ initially calculated by Pan & Oka (1986) has been superseded by more accurate ab initio calculations by Neale et al. (1996). Values from their extensive line lists extracted by Lindsay & McCall (2001) are given in Table 1. Since the background radiative temperature of 2.7 K is very much lower than any of the transition

TABLE 1
FREQUENCIES AND EINSTEIN COEFFICIENTS OF FORBIDDEN ROTATIONAL TRANSITIONS

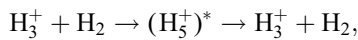
$J, K \rightarrow J, K (i \rightarrow f)$	Freq. (cm ⁻¹)	A_{if} (s ⁻¹)	$J, K \rightarrow J, K (i \rightarrow f)$	Freq. (cm ⁻¹)	A_{if} (s ⁻¹)	$J, K \rightarrow J, K (i \rightarrow f)$	Freq. (cm ⁻¹)	A_{if} (s ⁻¹)
4, 4→3, 1.....	7.255	2.78E-09	5, 0→5, 3.....	190.756	6.80E-04	7, 2→6, 1.....	501.093	1.05E-02
7, 6→6, 3.....	9.261	6.22E-08	3, 0→3, 3.....	201.524	7.40E-05	8, 3→8, 6.....	533.460	2.09E-02
7, 4→8, 7.....	29.655	3.59E-06	10, 6→9, 9.....	211.586	9.22E-04	6, 1→5, 2.....	553.791	5.37E-03
4, 2→5, 5.....	39.453	1.10E-06	8, 5→7, 2.....	220.891	1.98E-03	7, 3→7, 6.....	555.500	9.93E-03
6, 5→5, 2.....	51.347	6.38E-06	7, 4→6, 1.....	261.550	1.93E-03	8, 2→7, 1.....	568.013	2.59E-02
8, 1→8, 2.....	56.563	5.94E-05	4, 2→3, 1.....	273.701	1.80E-04	6, 3→6, 6.....	581.450	3.00E-03
7, 1→7, 2.....	58.880	4.19E-05	8, 1→8, 4.....	286.320	6.35E-03	5, 0→4, 3.....	612.525	3.03E-03
6, 1→6, 2.....	61.101	2.68E-05	7, 1→7, 4.....	298.423	4.05E-03	7, 1→6, 2.....	621.074	1.47E-02
5, 1→5, 2.....	63.197	1.53E-05	6, 3→5, 0.....	306.088	3.18E-03	8, 4→8, 7.....	666.334	2.19E-02
4, 1→4, 2.....	65.107	7.27E-06	6, 1→6, 4.....	310.199	2.25E-03	8, 1→7, 2.....	683.456	3.44E-02
3, 1→3, 2.....	66.758	2.64E-06	5, 1→5, 4.....	321.347	1.00E-06	7, 4→7, 7.....	700.315	6.80E-03
2, 1→2, 2.....	68.062	5.66E-07	3, 1→2, 2.....	325.482	3.51E-05	7, 0→6, 3.....	743.039	3.25E-02
5, 3→6, 6.....	84.606	1.81E-05	4, 1→4, 4.....	331.549	2.81E-04	5, 1→4, 4.....	748.280	7.51E-04
5, 4→4, 1.....	95.383	2.16E-05	8, 4→7, 1.....	338.256	7.00E-03	6, 1→5, 4.....	811.941	4.22E-03
8, 6→7, 3.....	100.112	1.65E-04	5, 2→4, 1.....	353.533	9.73E-04	8, 5→8, 8.....	815.622	1.35E-02
2, 2→1, 1.....	105.173	4.26E-07	4, 1→3, 2.....	405.563	3.23E-04	7, 1→6, 4.....	870.172	1.41E-02
6, 4→7, 7.....	128.566	9.85E-05	8, 2→8, 5.....	406.002	1.38E-02	8, 1→7, 4.....	922.999	3.58E-02
7, 5→6, 2.....	138.350	2.70E-04	7, 2→7, 5.....	423.844	8.00E-03	6, 2→5, 5.....	950.783	1.75E-03
4, 3→3, 0.....	141.847	5.97E-05	6, 2→5, 1.....	429.493	3.62E-03	7, 2→6, 5.....	1003.537	9.00E-03
7, 5→8, 8.....	170.887	3.40E-04	6, 2→6, 5.....	441.343	3.72E-03	8, 2→7, 5.....	1050.737	2.57E-02
7, 0→7, 3.....	178.278	2.13E-03	8, 3→7, 0.....	455.294	3.15E-02	7, 3→6, 6.....	1146.211	3.34E-03
6, 4→5, 1.....	180.395	3.36E-04	5, 2→5, 5.....	458.093	1.08E-03	8, 3→7, 6.....	1189.072	1.63E-02
3, 2→2, 1.....	190.662	1.76E-05	5, 1→4, 2.....	481.837	1.57E-03	8, 4→7, 7.....	1336.994	5.61E-03

NOTE.—Values from the extensive line list given by Neale et al. (1996) and extracted by Lindsay & McCall (2001) are used. Values for 4, 2 → 3, 1 and 10, 6 → 9, 9 are added.

frequencies, absorption and induced emission of H₃⁺ are neglected, and only the spontaneous emission is considered.

3.2. Collisional Process

Unlike the radiative process, collisional processes do not obey selection rules so rigorously. This is particularly true for H₃⁺, whose collision with H₂,



is actually a chemical reaction in which the five protons are scrambled, and even ortho ↔ para conversions occur (Uy et al. 1997; Cordonnier et al. 2000; Oka 2004). The energy of the activated complex (H₅⁺)^{*} is at least ~2000 cm⁻¹ above the lowest energy of H₃⁺ (Yamaguchi et al. 1987), and this excess energy is sufficient to make the protons scramble during a short time. The large rate constants for reactions between various isotopomers of H₃⁺ and H₂ (Anicich & Huntress 1986; Giles et al. 1992) and those at low temperatures (Gerlich 1993) demonstrate that the scrambling of nuclei occurs efficiently. Thus, collisional processes involving H₃⁺ are qualitatively different from those of neutral molecules such as H₂, H₂O, and NH₃, where conversions between ortho and para spin species are highly forbidden (Oka 1973). In addition, collisions involving H₃⁺ have much larger cross sections than those with neutral molecules because of the long range r^{-4} Langevin potential, instead of the weaker r^{-6} van der Waals potential. Such strong collisions tend to have random selection rules (Oka 1973). Here we take advantage of this fact and make a simplifying assumption of complete randomness, that is, collisional transitions without *any* selection rules, used by Van Vleck & Weisskopf (1945) for the extreme case of strong collisions. In actuality, there exist some nuclear spin selection

rules (Uy et al. 1997; Cordonnier et al. 2000; Oka 2004), but these and other subtleties related to energies and angular momenta are neglected in this paper.

With this assumption, the only guiding principle is the principle of detailed balancing,

$$\frac{k_{JK}^{J'K'}}{k_{J'K'}^{JK}} = \frac{g_{JK}}{g_{J'K'}} \exp\left(-\frac{E_{JK} - E_{J'K'}}{kT}\right), \quad (1)$$

where $k_{JK}^{J'K'}$ is the rate constant for collisional transitions from the initial level (J', K') to the final level (J, K), g_{JK} and E_{JK} are the statistical weight and the energy of the (J, K) level, respectively, and T is the kinetic temperature of the cloud. Based on the assumption of complete randomness of collisional processes, we decompose equation (1) as

$$k_{JK}^{J'K'} = C_{JK}^{J'K'} \sqrt{\frac{g_{JK}}{g_{J'K'}}} \exp\left(-\frac{E_{JK} - E_{J'K'}}{2kT}\right), \quad (2)$$

with

$$C_{JK}^{J'K'} = C_{J'K'}^{JK} = C \left\{ 1 + \sum_{J''K''} \left(\frac{g_{J''K''}}{\sqrt{g_{JK}g_{J'K'}}} \right)^{1/2} \times \exp\left[-\frac{E_{J''K''} - (1/2)(E_{JK} + E_{J'K'})}{2kT}\right] \right\}^{-1}, \quad (3)$$

where C is a constant independent of (J, K) and (J', K') whose value we set to the typical value of the Langevin rate constant, 2×10^{-9} cm³ s⁻¹. The summation does not include JK and $J'K'$. The expression in the curly braces of equation (3) is an

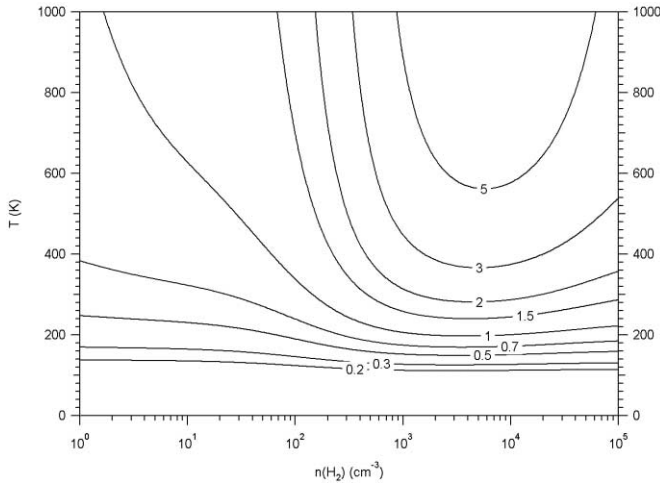


FIG. 2.—Values of the calculated population ratios $n(3, 3)/n(1, 1)$ as a function of H_2 number density $n(H_2)$ and kinetic temperature T .

average normalizing factor that normalizes $C_{JK}^{J'K'}$ and $C_{J'K'}^{JK}$, keeping equation (1) intact. Note that equation (2) is the only way to decompose equation (1) symmetrically with respect to (J, K) and (J', K') . We do not find this formula in the literature, but we believe that this formula gives the essential characteristics of reactive collisional processes involving H_3^+ .

3.3. Steady State

The steady state, relative populations of H_3^+ are obtained from simultaneous equations,

$$\frac{dn(JK)}{dt} = \sum_{J'K'} \left[A_{JK}^{J'K'} n(J'K') - A_{J'K'}^{JK} n(JK) \right] + \sum_{J'K'} \left[k_{JK}^{J'K'} n(J'K') - k_{J'K'}^{JK} n(JK) \right] n(H_2) = 0, \quad (4)$$

where $A_{JK}^{J'K'}$ denotes the Einstein coefficient for spontaneous emission $(J', K') \rightarrow (J, K)$, $E_{J'K'} > E_{JK}$ is required for the first term, and $E_{JK} > E_{J'K'}$ for the second, while for $k_{J'K'}^{JK}$, the energy relation of the initial level (J', K') and the final level (J, K) is arbitrary.

Relative populations have been calculated for all levels as a function of the two variables in equation (4), that is, the H_2

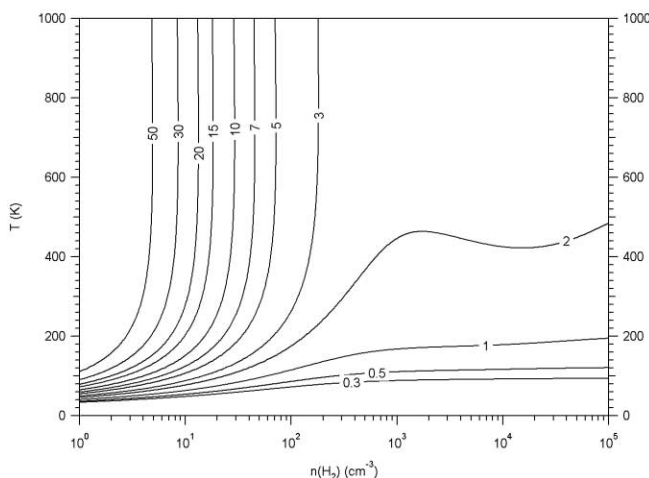


FIG. 3.—Plots of $n(3, 3)/n(2, 2)$ as a function of $n(H_2)$ and T .

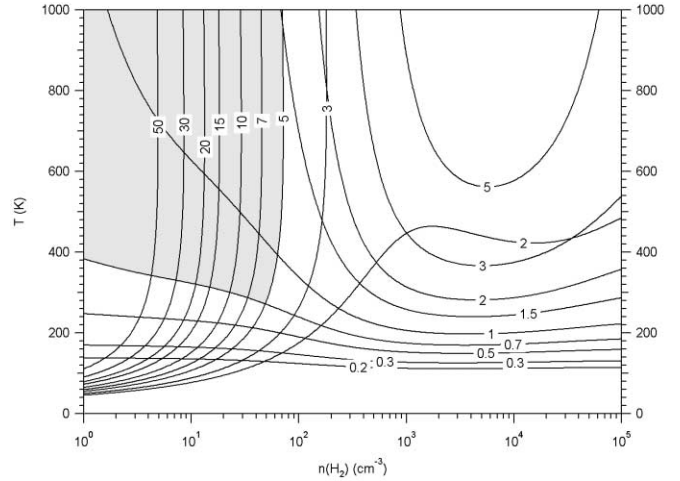


FIG. 4.—Figs. 2 and 3 combined, in which the conditions corresponding to the preliminary observed values of $n(3, 3)/n(1, 1) = 1_{-0.3}^{+0.5}$ and $n(3, 3)/n(2, 2) \geq 5$ are shown by the shaded area.

number density $n(H_2)$ and temperature T , which is implicit in $k_{J'K'}^{JK}$ according to equation (2). Rotational levels up to $(J, K) = (9, 8)$, which is 2396 cm^{-1} above the $(1, 1)$ level, have been included in the calculation. We pay special attention to relative populations involving the metastable $(3, 3)$ level, in particular $n(3, 3)/n(1, 1)$ and $n(3, 3)/n(2, 2)$, which have been observed to be ~ 1 (Goto et al. 2002) and more than 5 (T. R. Geballe & T. Oka 2004, in preparation), respectively, toward GCS 3-2. Calculated values of $n(3, 3)/n(1, 1)$ and $n(3, 3)/n(2, 2)$ are shown in Figures 2 and 3, respectively.

4. DISCUSSIONS

4.1. Accuracy

Three assumptions employed in these model calculations are (1) the steady state approximation, (2) the Einstein coefficients listed in Table 1, and (3) the collisional rate constants given in equation (2). Justification for assumption 1 was given at the beginning of § 3. The inaccuracy introduced by this assumption is estimated to be on the order of a few percent. The Einstein coefficients given by Neale et al. (1996) are very accurate, and their errors are negligible (note, however, that the values by Miller & Tennyson [1988] are too large by a factor of $2J + 1$).

Clearly, the major source of inaccuracy in this model calculation is the formula for collisional rate constants given in equations (2) and (3). The assumption of a completely random collision, the decomposition of detailed balancing into a rate constant of the form in equation (2), and the normalization of the collision rate to the Langevin rate constant for ion-neutral reactions all introduce errors. More rigorous quantum mechanical calculations of the individual collision rates are awaited. Collisions with atomic hydrogen should also be considered for a very low density cloud. Nevertheless, we believe that our calculated results represent the essential characteristics of the H_3^+ thermalization and can be used for the analysis of observed data and for assessing the observability of H_3^+ in metastable rotational levels higher than $(3, 3)$.

4.2. $(3, 3)$ and Higher Metastable Levels

A simultaneous plot of Figures 2 and 3 is given in Figure 4, in which the region of conditions that gives the preliminary observed values of $n(3, 3)/n(1, 1) \sim 1_{-0.3}^{+0.5}$ and $n(3, 3)/n(2, 2) >$

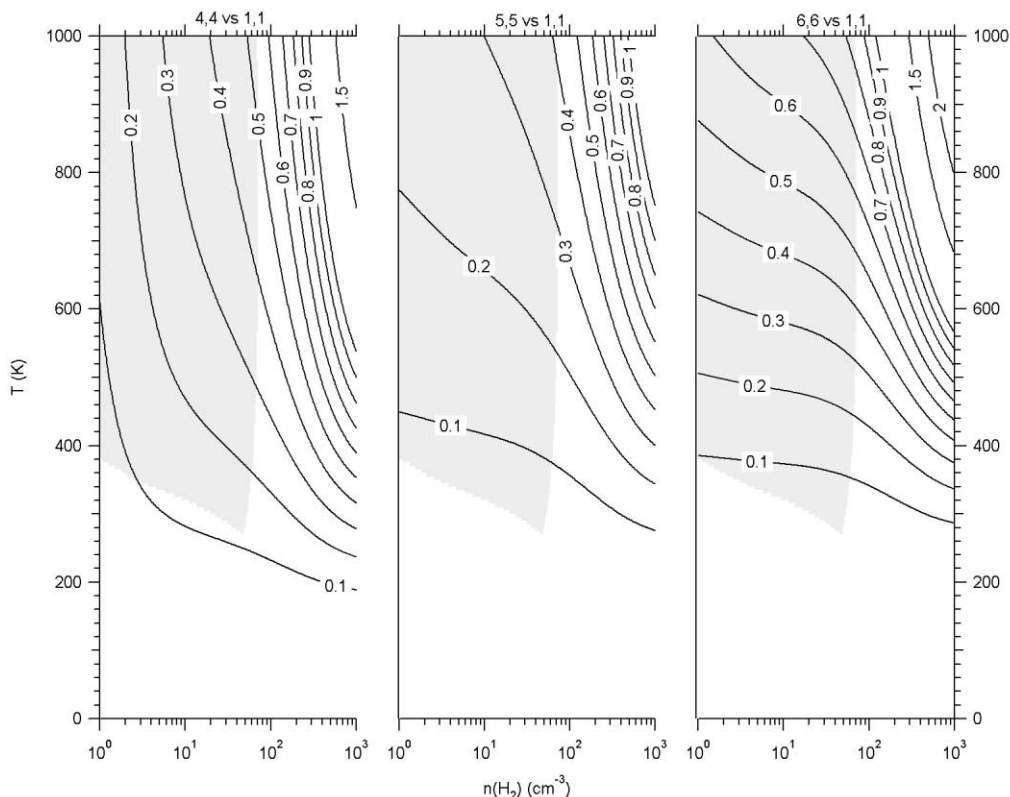


FIG. 5.—Plots of $n(4, 4)/n(1, 1)$, $n(5, 5)/n(1, 1)$, and $n(6, 6)/n(1, 1)$ as functions of $n(\text{H}_2)$ and T . They indicate the possibility of observing H₃⁺ in those metastable levels higher than (3, 3).

5 are indicated as a shaded area. It is seen that those conditions are met by high-temperature ($T \geq 300$ K), low-density [$n(\text{H}_2) \leq 70 \text{ cm}^{-3}$] clouds. In order to assess the possibility of observing H₃⁺ in other metastable or quasi-metastable levels, the values $n(4, 4)/n(1, 1)$, $n(5, 5)/n(1, 1)$, and $n(6, 6)/n(1, 1)$ were calculated and are shown in Figure 5. The qualitatively different behavior of $n(4, 4)$ as opposed to $n(5, 5)$ and $n(6, 6)$ at very low H₂ density is due to its quasi metastability. These results indicate that the higher $J = K$ levels may have an observable H₃⁺ population. Observations of more metastable levels will give tighter constraints on the conditions of the clouds.

The detectability of the higher metastable levels depends also on the strength of the transition dipole moment, $|\mu_{if}|^2$. Frequencies and strengths of transitions possibly useful for observations are listed in Table 2. Note that the strength of the $R(1, 1)^l$ transition, $|\mu_{if}|^2 = 0.0141 \text{ D}^2$, is lower than those of other $R(J, J)^l$ transitions, and this makes the detection of metastable H₃⁺ easier than calculated from their population ratios. Unfortunately, the $R(6, 6)^l$ line overlaps with the Q -branch of the CH₄ ν_3 band, which makes the atmosphere almost completely opaque. For observation of H₃⁺ in the (6, 6) metastable level, the best choice is the $^lR(6, 6)$ line of the $2\nu_2$

TABLE 2
FREQUENCIES AND INTENSITIES OF SPECTRAL LINES RELEVANT FOR THE ANALYSIS OF METASTABLE ROTATIONAL LEVELS

Transition	Freq. (cm ⁻¹)	$ \mu ^2$ (D ²)	Transition	Freq. (cm ⁻¹)	$ \mu ^2$ (D ²)
$R(6, 6)^u$	3182.038	0.00525	$Q(3, 3)$	2561.497	0.00648
$R(5, 5)^u$	3096.416	0.00555	$Q(2, 2)$	2554.666	0.00860
$R(6, 6)^l$	3014.364	0.02018	$Q(1, 1)$	2545.420	0.01282
$R(4, 4)^u$	3008.108	0.00612	$Q(1, 0)$	2529.724	0.02535
$R(5, 5)^l$	2956.073	0.02006	$^nP(5, 5)$	4987.419	0.00221
$R(3, 3)^l$	2918.026	0.00708	$^nP(4, 4)$	4984.337	0.00254
$R(4, 4)^l$	2894.488	0.01975	$^nP(6, 6)^l$	4975.338	0.00142
$R(3, 3)^l$	2829.925	0.01923	$^nP(3, 3)$	4971.561	0.00258
$R(2, 2)^u$	2823.138	0.00943	$^lR(1, 1)$	4968.272	0.00396
$R(2, 2)^l$	2762.070	0.01776	$^nP(2, 2)$	4955.991	0.00228
$R(1, 1)^u$	2726.220	0.01579	$^lR(2, 2)$	4936.000	0.00415
$R(1, 0)$	2725.898	0.02588	$^lR(3, 3)$	4900.393	0.00434
$R(1, 1)^l$	2691.443	0.01407	$^lR(4, 4)$	4861.790	0.00455
$Q(6, 6)$	2573.582	0.00376	$^lR(5, 5)$	4820.598	0.00477
$Q(5, 5)$	2571.118	0.00437	$^lR(6, 6)$	4777.226	0.00502
$Q(4, 4)$	2567.288	0.00522			

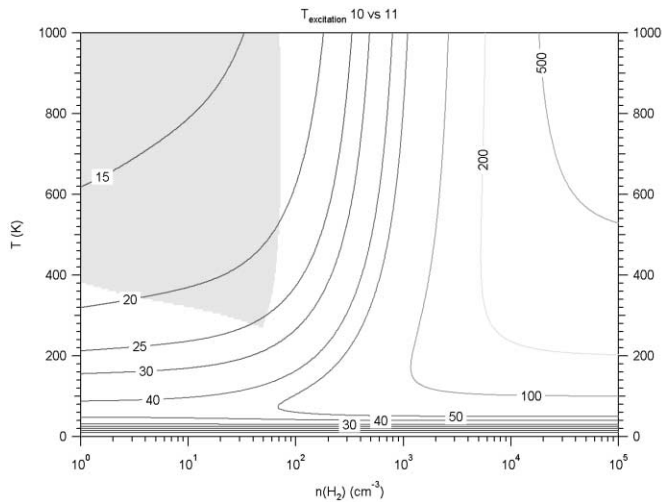


FIG. 6.—Excitation temperatures determined from the calculated $n(1, 0)/n(1, 1)$ as a function of $n(\text{H}_2)$ and T . Note that for low $n(\text{H}_2)$, the excitation temperatures cannot be higher than 50 K, even in high-temperature clouds.

overtone band, which is 4 times weaker than the $R(6, 6)^l$ of the fundamental.

4.3. Excitation Temperature from $n(1,0)/n(1,1)$

Of special interest is the excitation temperature of H_3^+ in the lowest ortho level (1, 0), determined from the relative population $n(1, 0)/n(1, 1) = 2 \exp(-32.9/T_{\text{ex}})$. This temperature has been assumed to represent the temperature of the clouds (Geballe & Oka 1996; Geballe et al. 1999; McCall et al. 1998, 1999, 2003). Figure 6 shows the excitation temperature determined from the model calculation of $n(1, 0)/n(1, 1)$ as a function of the density and temperature of the clouds. It is noted that the excitation temperature is always lower than the cloud temperature, except for the low-temperature region, where it is very nearly equal to the cloud temperature. At a higher temperature, the ortho- H_3^+ in the (1, 0) level is pumped to the (2, 1) and (2, 2) para levels by reactive collisions and is rapidly cooled to the (1, 1) level by spontaneous emission leading to a low excitation temperature. This effect is very pronounced in the low-density region. When $n(\text{H}_2)$ is lower than 70 cm^{-3} , the excitation temperature cannot be higher

than 50 K, regardless of the cloud temperature. Thus, the discrepancy between the low H_3^+ excitation of 23 K for the diffuse cloud toward ζ Per reported by McCall et al. (2003) and the higher H_2 excitation temperature of 58 K for the same cloud, calculated from the column densities of $J = 1$ and $J = 0$ H_2 reported by Savage et al. (1977), may be at least partly explained.

This effect is even more spectacular at low density and high temperature, especially in the shaded area in Figure 6. This shows that the very low H_3^+ excitation temperature of $T_{\text{ex}} < 30$ K, calculated from the level column densities N_{level} listed in Table 3 of Goto et al. (2002), is compatible with the high cloud temperature $T > 300$ K indicated by the observation of H_3^+ in the (3, 3) metastable level. A future accurate determination of the (1, 0) excitation temperature will provide a crucial piece of information on the cloud conditions.

It was pointed out by the referee that electron impact rotational excitation or de-excitation of H_3^+ through the strong, long-range r^{-3} potential between the electron charge and the H_3^+ quadrupole moment may play a significant role in thermalization, especially at low temperatures. According to Faure & Tennyson (2002, 2003), rate constants of such processes amount to $10^{-7} \text{ cm}^3 \text{ s}^{-1}$ depending on temperature, values that are comparable to that of dissociative recombination. Thus, since the hydrogen number density is 4 orders of magnitude higher than that for electrons, the electron effect for thermalization is 2 orders of magnitude less than that of H and H_2 . For molecular ions such as HCO^+ with a large dipole moment (~ 4 D), the stronger, longer range r^{-2} charge-dipole interaction makes the rate 2 orders of magnitude higher than for H_3^+ (Faure & Tennyson 2001), and the contribution of electrons to thermalization becomes comparable to that of H and H_2 . This problem is also related to the relative rate of impact rotational (de-)excitation and dissociative recombination. Future observation of H_3^+ may provide information for the latter, which is currently controversial (McCall et al. 2003).

We are grateful to B. J. McCall and J. K. G. Watson for reading this paper. We also wish to thank the anonymous referee for the comment discussed above. This work has been supported by NSF grant PHY 00-99442.

REFERENCES

- Anicich, V. G., & Huntress, W. T., Jr. 1986, *ApJS*, 62, 553
 Black, J. H. 1998, *Faraday Discuss.*, 109, 257
 Cordonnier, M., Uy, D., Dickson, R. M., Kerr, K. E., Zhang, Y., & Oka, T. 2000, *J. Chem. Phys.*, 113, 3181
 Faure, A., & Tennyson, J. 2001, *MNRAS*, 325, 443
 ———. 2002, *J. Phys. B*, 35, 3945
 ———. 2003, *MNRAS*, 340, 468
 Geballe, T. R., McCall, B. J., Hinkle, K. H., & Oka, T. 1999, *ApJ*, 510, 251
 Geballe, T. R., & Oka, T. 1996, *Nature*, 384, 334
 Gerlich, D. 1993, *J. Chem. Soc. Faraday Trans. 1*, 89, 2199
 Giles, K., Adams, N. G., & Smith, D. 1992, *J. Phys. Chem.*, 96, 7645
 Goldsmith, P. F. 1972, *ApJ*, 176, 597
 Goto, M., McCall, B. J., Geballe, T. R., Usuda, T., Kobayashi, N., Terada, H., & Oka, T. 2002, *PASJ*, 54, 951
 Green, S., & Chapman, S. 1978, *ApJS*, 37, 169
 Herbst, E., & Klemperer, W. 1973, *ApJ*, 185, 505
 Lindsay, M. C., & McCall, B. J. 2001, *J. Mol. Spectrosc.*, 210, 60
 McCall, B. J., Geballe, T. R., Hinkle, K. H., & Oka, T. 1998, *Science*, 279, 1910
 ———. 1999, *ApJ*, 522, 338
 McCall, B. J., et al. 2002, *ApJ*, 567, 391
 ———. 2003, *Nature*, 422, 500
 Miller, S., & Tennyson, J. 1988, *ApJ*, 335, 486
 Neale, L., Miller, S., & Tennyson, J. 1996, *ApJ*, 464, 516
 Oka, T. 1973, *Adv. At. Mol. Phys.*, 9, 127
 ———. 2004, *J. Mol. Spectrosc.*, in press
 Oka, T., Shimizu, F. O., Shimizu, T., & Watson, J. K. G. 1971, *ApJ*, 165, L15
 Pan, F.-S., & Oka, T. 1986, *ApJ*, 305, 518
 Savage, B. D., Bohlin, R. C., Drake, J. F., & Budich, W. 1977, *ApJ*, 216, 291
 Uy, D., Cordonnier, M., & Oka, T. 1997, *Phys. Rev. Lett.*, 78, 3844
 Van Vleck, J. H., & Weisskopf, V. F. 1945, *Rev. Mod. Phys.*, 17, 227
 Watson, J. K. G. 1971, *J. Mol. Spectrosc.*, 40, 536
 Watson, W. D. 1973, *ApJ*, 183, L17
 Yamaguchi, Y., Gaw, J. F., Remington, R. B., & Shaefer, H. F., III. 1987, *J. Chem. Phys.*, 86, 5701